Organic Optoelectronic Devices Based on Through-Space Interaction

Jiaqi Peng,[a] Liyuan Hou,[a] Dan Liu,[a] Zheng Zhao,[a] Jianquan Zhang,[a,*] Zijie Qiu,[a,c,*] Ben Zhong Tang[a,b,*]

[a] School of Science and Engineering, Shenzhen Institute of Aggregate Science and Technology, The Chinese University of Hong Kong, Shenzhen (CUHK-Shenzhen), Guangdong 518172, China

[b] Department of Chemistry, Hong Kong Branch of Chinese National Engineering Research Center for Tissue Restoration and Reconstruction, The Hong Kong University of Science and Technology, Kowloon, Hong Kong, China

[c] Max Planck Institute for Polymer Research, Ackermannweg 10, 55128 Mainz, Germany

Keywords: Through-space interaction, organic fluorescent film sensor, organic light-emitting diodes, single-molecule wires, photoswitches

Abstract: Through-space interaction (TSI), including through-space conjugation (TSC) and through-space charge transfer (TSCT), has emerged as a promising strategy for designing functional materials and constructing superior optoelectronic devices. Because of the multichannel charge transport and structural flexibility, TSI-based devices often exhibit high-performance optoelectronic properties, such as excellent photoluminescence,

high charge carrier mobility, and outstanding device efficiency. In this review, the principles and characteristics of TSI are briefly introduced. Then we mainly focused on the recent progress of optoelectronic device applications based on materials with TSC and TSCT. Various advanced optoelectronic devices, including organic fluorescence film sensors, organic light-emitting diodes, single-molecule junctions, and photoswitches are discussed in detail and possible breakthroughs are proposed for future molecular design and efficiency enhancement.

1. Introduction

Organic π-conjugated materials have attracted a lot of attention and have been widely used in organic optoelectronic devices.[1-5] The π-units in most π-conjugated materials are connected by covalent bonds or fused aromatics,[6-9] where electron delocalization and charge separation happen. Besides, non-covalent interactions between aromatic rings can produce effective electron interactions between closely packed aromatic rings and/or lone electron pairs, which is also known as through-space interaction (TSI).[10-12] It is widely used to regulate the photophysical properties of optoelectronic materials, such as emission color, charge transport ability, and luminescence efficiency.[12-15] In addition, the twisted structures of the molecules with TSI can prevent close intermolecular π–π stacking and subsequent emission quenching effect in the aggregated and solid state.[16-19]

TSI can occur intermolecularly, which is commonly utilized in regulating optoelectronic properties of crystals and aggregates.[20-22] On the other hand, intramolecular TSI is observed

in molecules possessing aromatic rings with a preferably face-to-face orientation by different bridging units.[20, 23, 24] The studies of the intramolecular TSI can be further specified as (1) through-space conjugation (TSC), where uniform delocalization of π-electrons are emphasized; (2) through-space charge transfer (TSCT), where separations of frontier orbitals between the spatially adjacent donor (D) and acceptor (A) groups are essential (**Figure 1**). In view of photophysics, the investigations of TSCT focus more on the D-A charge transfer in the excited states.

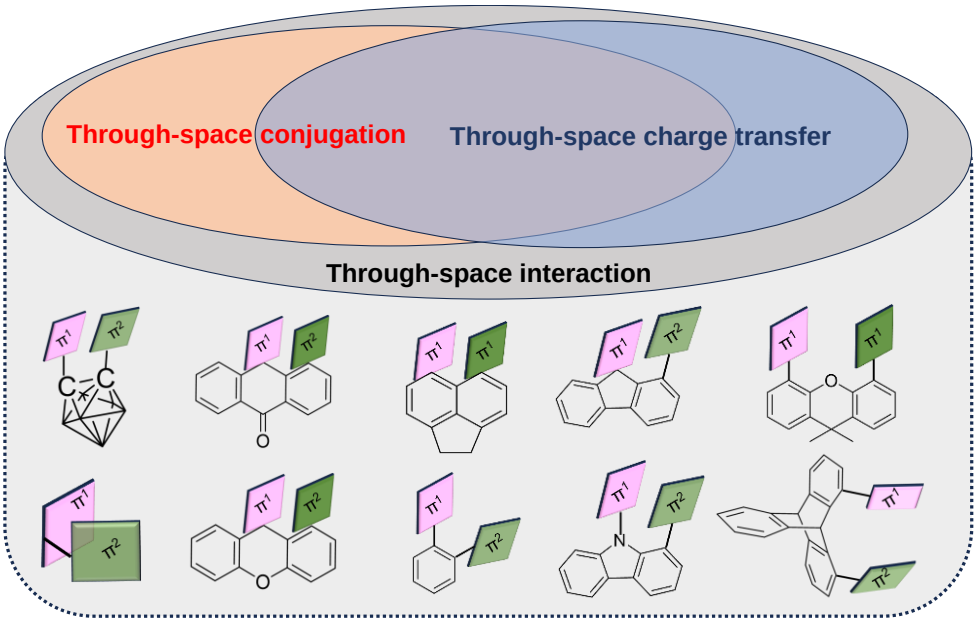

Figure 1. The relationship among through-space interaction (TSI), through-space conjugation (TSC), and through-space charge transfer (TSCT). Below are several kinds of architectures.

Compared to conventional through-bond conjugation and charge transfer,[25, 26] TSI is more sensitive to the spatial distance and the degree of overlapping, which can be subtly

regulated by different states (e.g. gas, dissolved, aggregated, or crystalline states) and microenvironment (e.g. polarity, temperature, etc.). Additionally, the highly twisted structures can strengthen intramolecular noncovalent interactions between D and A moieties, leading to reduced nonradiative decays and improved device performance with minimal efficiency roll-off. Therefore, organic functional materials with TSI have become a hotspot in various optoelectronic applications.

In this review, we focus on the recent progress of device applications of organic functional materials with intriguing intramolecular TSI. Organic fluorescent film sensors (OFFSs), organic light-emitting diodes (OLEDs), single-molecule junctions, and photoswitches are discussed in detail. In outlook and perspectives, we summarize the design principles and advantages of organic optoelectronic devices based on TSI.

2. Device Applications of TSI-based Materials

2.1 Organic Fluorescent Film Sensor

Fast, selective, real-time, and sensitive detection of alkane is significant and challenging to environmental and occupational safety. OFFSs are considered a promising choice for the required vapor monitoring. Therefore, the performance of an OFFS is largely determined by the innovative design of sensing fluorophore and optimization of adlayer structure. TSCT molecular systems generally possess a rigid U-shaped configuration, where the donor and the acceptor are in face-to-face alignment at a precisely controlled distance. For gas sensing, this intriguing non-planar molecular structure would generate a significant

amount of voids in the thin film layer due to the packing of the sensing fluorophores, which is a prerequisite for fast and reversible sensing. Furthermore, the twisted molecular structure and poor packing also provide the necessary space to accommodate analyte molecules, thereby altering of excited state characteristics of the sensing fluorophores. Therefore, TSCT molecular systems may be promising candidates for sensing fluorophores to address challenging alkanes.

In 2022, Fang *et al* chose o-carborane as a molecular scaffold to connect PBI and anthracene (AN) to establish a U-shaped TSCT molecular system (**Figure 2**).[27] The interlocked, face-to-face alignment between the donor and acceptor favors the mass transport of volatile organic compounds (VOCs) in the film state. The fabricated OFFS showed an experimental detection limit of ~10 ppm for *n*-pentane with less than 5 s detection time. Meanwhile, the sensor is small (~3.7 cm^3), power-saving, and workable at room temperature. Therefore, such an on-site and real-time gas monitoring technique with negligible interference reveals the effectiveness of the design strategy. It is the first and only report of a high-performance OFFS for the alkanes with TSCT molecule as the sensing fluorophore until now. Considering their great potential, it is anticipated that more TSCT-based OFFSs will be investigated and reported in the near future.

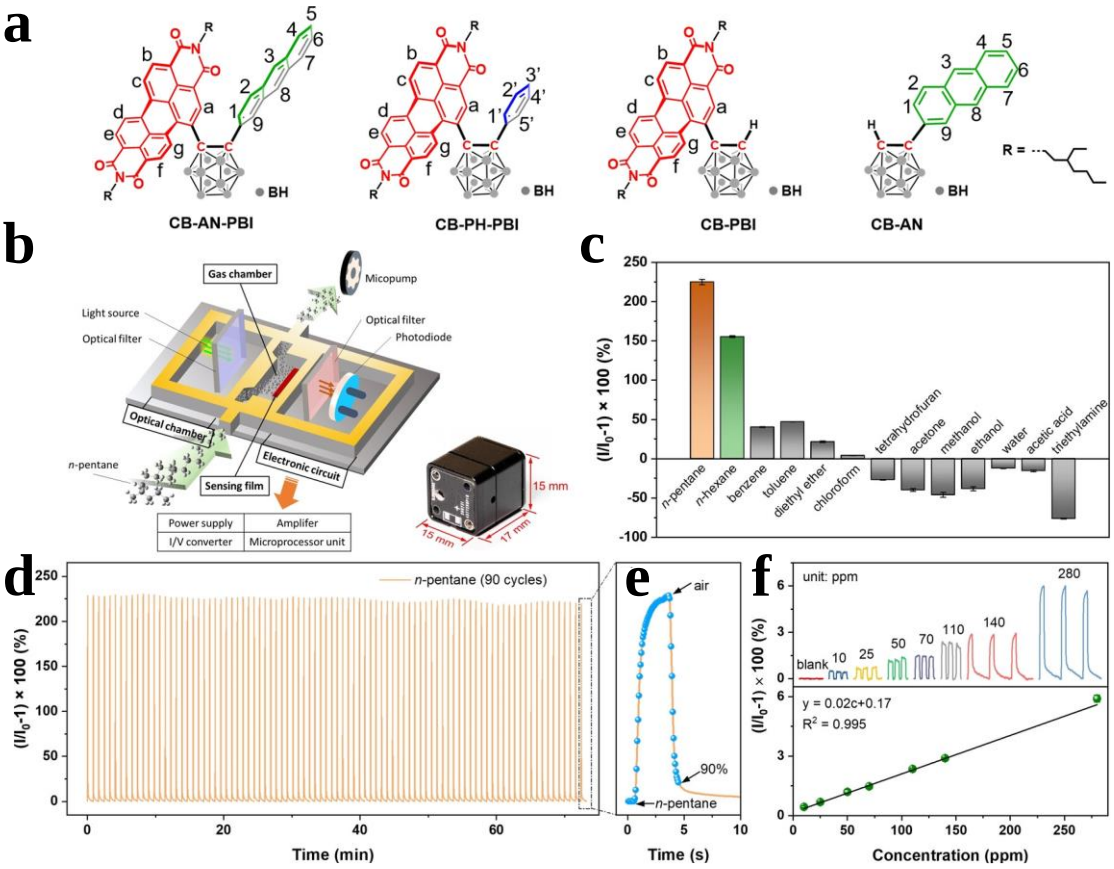

Figure 2. (a) The molecular structures of CB-AN-PBI, CB-PH-PBI, CB-PBI and CB-AN. (b) Schematic description of the sensory unit of the home-made sensing platform. Inset: Photograph of the sensory unit. (c) Fluorescence responses of the CB-AN-PBI-based film sensor to n-pentane, n-hexane, and various potential interferences, error bars represent the standard deviation of five measurements. (d) Real-time responses of CB-AN-PBI-based film sensor to saturated n-pentane in more than 90 repeated sensing cycles at 298 K. e) An enlarged sensing cycle for analysis of the response and recovery time. (f) Fluorescence responses of CB-AN-PBI-based film sensor to n-pentane at different vapor concentrations, where each measurement was repeated three times (upper). The experimentally obtained and linearly fitted responses of CB-AN-PBI-based film sensor to n-pentane at different

vapor concentrations (bottom) from ref.[27] Copyright 2022 American Chemical Society.

2.2 Organic Light-Emitting Diodes

The third-generation OLEDs based on thermally activated delayed fluorescence (TADF) are expected to be widely used in lighting, smartphones, flat panel displays, and flexible displays owing to efficient exciton utilization and luminescence quantum yields.[28-37] In this regard, TSCT-based TADF emitters are one of the most promising luminescent materials because the spatial interaction that occurs between the D and A can result in a very small ΔE_{ST} and limited rotation.[38, 39] Therefore, it is beneficial to realize fast reverse intersystem crossing (RISC) and fabricate high-performance OLEDs by changing the donor and acceptor units and controlling their relative positions.[40]

In 2017, Swager and Baldo *et al.*[11] designed and synthesized three D-A molecules with a U-shape TSCT structure. The crystal structures confirmed the cofacial arrangement of the donor and acceptor groups at distances (3.3-3.5 Å), which allowed for efficient CT without producing a strong ground state π interaction (**Figure 3a**). Moreover, typical Aggregation-Induced Emission (AIE) properties of these materials were observed (**Figure 3b**). To explore the device fabrication and evaluation, XPT and XtBuCT were used as emissive dopants in OLED devices by vacuum evaporation process. The device architecture and performance are shown in **Figures 3c and 3d**. The electroluminescence (EL) spectra displayed peaks at 584 nm for XPT and 488 nm for XtBuCT devices that were red-shifted relative to the photoluminescence (PL) determined in the toluene solution. The maximum

external quantum efficiency (EQE) of XPT devices was 10%, which exceeded the theoretical limit of 6% expected for a simple fluorescent OLED indicating XPT was efficiently converting triplet excitons into emission through the singlet pathway by the TADF mechanism (**Figure 3e**).

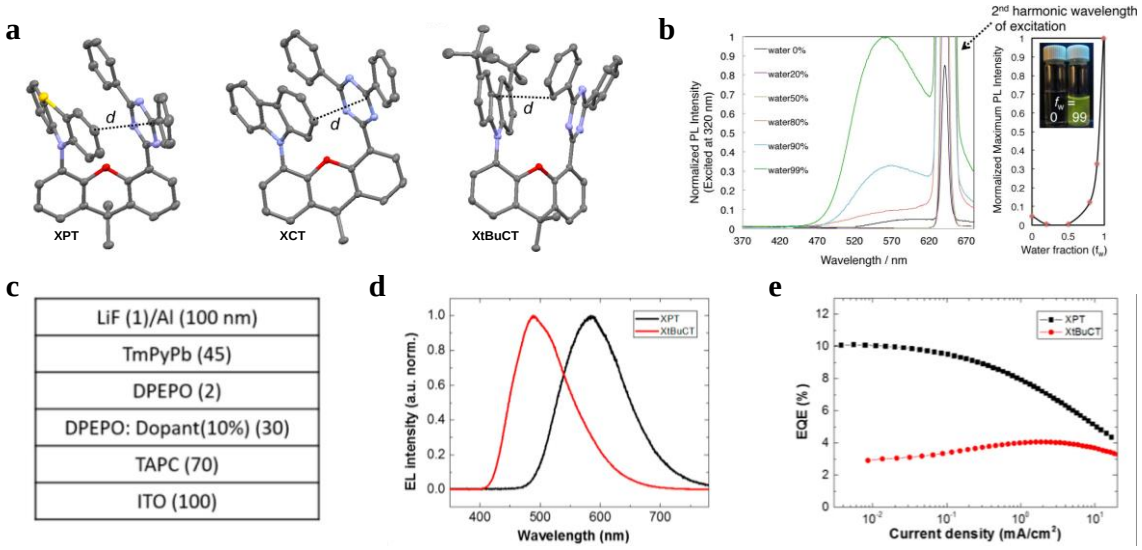

Figure 3. (a) Crystal structures of XPT (d = 3.423 Å), XCT (d = 3.375 Å), and XtBuCT (d = 3.299 Å). The d below each structure represents the distances shown by the black dashed lines from ref.[11] (b) PL spectra of XPT in THF/water mixture and the change of normalized PL peak intensity with different water fractions; inset: PL images of XPT with different water fractions under 365 nm UV light from ref.[11] (c) OLEDs device structure from ref.[11] (d) EL spectrum of the devices from ref.[11] (e) EQEs of the OLEDs as a function of current density from ref.[11] Copyright 2017, American Chemical Society.

Furthermore, OLEDs based on exciplexes have reached impressive EQEs exceeding 16% during the past few years.[41] Liao and Friend *et al.*[42] in 2020 proposed a TSCT molecular

design strategy to enhance exciplex-type TADF emission. As shown in **Figure 4a**, the donor and acceptor units were connected through rigid linkers, which confined them in a tightly arranged coplanar conformation. The optoelectronic performance of the OLEDs was tuned by changing the connection position and conjugation strength of the acceptors. Quantum-chemical calculations showed that the TSCT molecular design strategy is beneficial for the creation of an intramolecular exciplex with pure CT character. In order to fabricated OLED devices by solution processing techniques, TSCT molecules need to have good solubility. So Jiang and Xie *et al.*[14] introduced solubilizing groups to the C7-site of the bridge linker part and kept the other side of the fluorene away from the acceptors in 2021. The single-crystal structure shown in **Figure 4b** illustrated that for C6-DMB and tBu-DMB, the distances between the TRZ plane and the triphenylamine plane connected to the bridge fluorene are 3.03 and 3.05 Å, respectively, which were smaller than that of DM-B (3.16 Å). These DM-B derivatives have smaller D/A distances in a face-to-face manner, resulting in better spatial interactions. The maximum EQEs of the solution-processed devices with C6-DMB and tBu-DMB were 21.0% and 21.7% shown in **Figure 4c**. The results indicated that C6-DMB and tBu-DMB had outperformed the solution-processed TSCT TADF emitters.

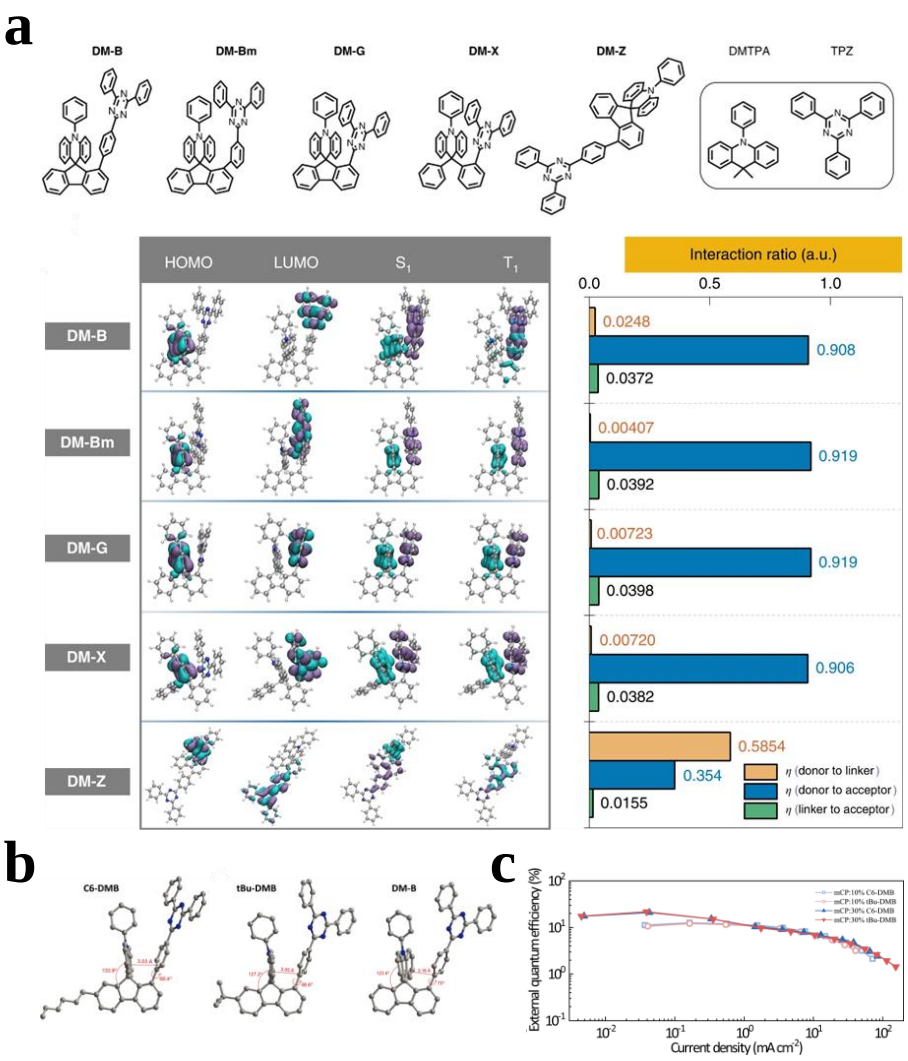

Figure 4. (a) Chemical structures of DM-B, DM-Bm, DM-G, DM-X and DM-Z and their molecular counterparts (DMTPA donor and TPZ acceptor); the distribution of the HOMOs and LUMOs and the analysis for the distribution of the hole (blue) and electron (purple) for S1 and T1; the contribution ratio (η) for the electron transition from donor to linker, donor to acceptor and linker to acceptor at the S1 excited state from ref.[42] (b) Crystal structures of C6-DMB, tBu-DMB, and DM-B from ref.[14] (c) EQE to current density curves of doped devices from ref.[14] Copyright 2020 2022, Nature.

To further explore efficient TSCT for TADF applications, Jiang *et al.*[43] first suggested the creation of a multilayer D/A/D conformation to ensure multiple TSCT. Multiple π-stacked molecules enabled more parallel D/A configurations through the introduction of additional donors, which yielded smaller singlet-triplet energy split (ΔE_{ST}), faster RISC processes, and higher device efficiencies (**Figure 5a**). As shown in **Figure 5b**, DM-BD1 exhibited a double-layer quasi-parallel structure in the D/A/D configuration. DM-BD2 possessed a typical sandwich D/A/D structure because the spatial site barrier does not allow for *cis*-conformations. DM-BD1 and DM-BD2 have almost perpendicular torsion angles of 81° and 87°, respectively, at the single bond connection between the fluorene bridge and the TPZ. Combined with the orthogonal spiro connection between the donor and the fluorene bridge, the TPA and TPZ units can form a face-to-face D/A spatial conformation. Compared to their previous work, both D/A/D-based DM-BD1 (28.0%) and DM-BD2 (26.2%) got higher EQEs than the D/A-based analogs DM-B (27.4%), and DM-Bm (21.7%) in **Figure 5b**. The DM-BD2-based device achieved a greater increase in EQE than DM-Bm because the dual donors in the sandwich conformation played a better role in maintaining a parallel face-to-face D/A/D conformation, which could further limit the free motion of each layer to prevent energy loss. DM-BD1 had a slight conformational change in D/A interactions compared to DM-B, but the EQE was still increased due to the shorter D/A distance induced by the additional donor. These device properties suggested that this multilayer molecule with TSCT and dense D/A/D was conducive to the realization of highly efficient devices. TADF molecules with multiple TSCT properties are scarce due to difficulties in molecular

design and synthesis.

Different from the molecular design of D/A/D structures, Tang and Li *et al.*[44] reported a simple and versatile method to construct a three-dimensional mismatched dislocation sandwich A-D-A conformation of TADF molecules with multiple TSCT properties in 2022. As shown in **Figure 5c**, the scaffold of 2PXZ-2TRZ had high structural rigidity, multiple TSCT, very small ΔE_{ST}, high photoluminescence quantum yields (Φ_{PL}), and fast RISC rate constants (k_{RISC}). Therefore, OLEDs employing the molecule as a dopant could achieve a maximum EQE of 27.1% and good efficiency stability at high brightness (**Figure 5d**). In addition, 2PXZ-2TRZ in the polymerized state allowed AIE, leading to a maximum EQE of up to 10.2% for the non-doped device. These results indicated that large PAHs with multilocked structures have great potential for efficient multiplexed TSCT-TADF emitters.

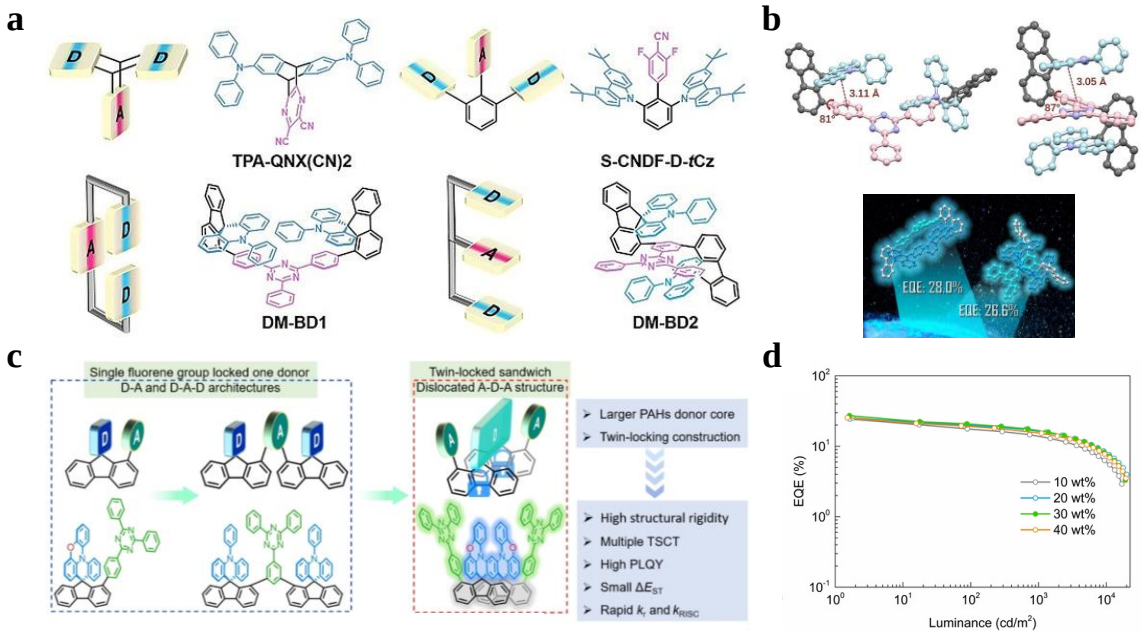

Figure 5. (a) Spatial D/A/D molecules of TPA-QNX(CN)2, S-CNDF-D-tCz, and DM-BD1, DM-BD2 from ref.[43] (b) Single-crystal structures (hydrogen atoms are omitted) of DM-

BD1 (left) and Dm-BD2 (right); EQE of DM-BD1 and DM-BD2 from ref.[43] (c) Representative TSCT-TADF materials and the design strategy for the dislocated twin-locking configuration from ref.[44] (d) EQE versus luminance of devices with various concentrations of 2PXZ-2TRZ doped into the PPF host from ref.[44] Copyright 2020 2022, Wiley.

At the same time, the differences between through-bond charge transfer (TBCT) and TSCT molecules in OLED were comparatively studied. Qiu *et al.*[45] designed a series of U-shaped TSCT molecules and L-shaped TBCT molecules to compare the effect of CT between different aromatic units on TADF,[5, 46] and second-order nonlinear optics (NLO). The U-shaped and L-shaped molecules are shown in **Figure 6a**. The experimental results showed that the U-shaped molecules emit delayed fluorescence in the solid state. Whereas the polarization effect led to an increase in the L-shaped compounds' hyperpolarizability values (β_{tot}) values, which was favorable to improving the performance of NLO applications. To have a clear understanding of the effects of TSCT and TBCT on the emitter PL and EL properties of OLED with TADF properties, a direct comparison between these two types emitters was carried out by Tang and Zhao *et al.*[23] The higher EQE and smaller efficiency roll-off, which is shown in **Figure 6b**, suggested that the introduction of TSCT may be more effective than linear TBCT in creating efficient TADF emitters, especially for molecules with long conjugated backbones, resulting in better EL performance. Zhu and Qi *et al.*[24] designed and developed a series of AIE-active TADF emitters adopting

triphenylamine as a donor and phenyl ketone as an acceptor unit were designed and developed as shown in **Figure 6c**. Via controlling the position of the donor and acceptor, the evolution of the charge transfer category from through-bond to through-space was achieved. Furthermore, in comparison with TBCT emitters, the TSCT displayed enhanced AIE properties due to the strongly suppressed non-radiative decay resulting from both highly twisted structures and restricted intramolecular motion between the donor and the acceptor. The comparative studies of these TSCT and TBCT molecules have advanced the further development of the theory of spatial conjugation and have shown them to be promising in a range of optoelectronic materials and devices.

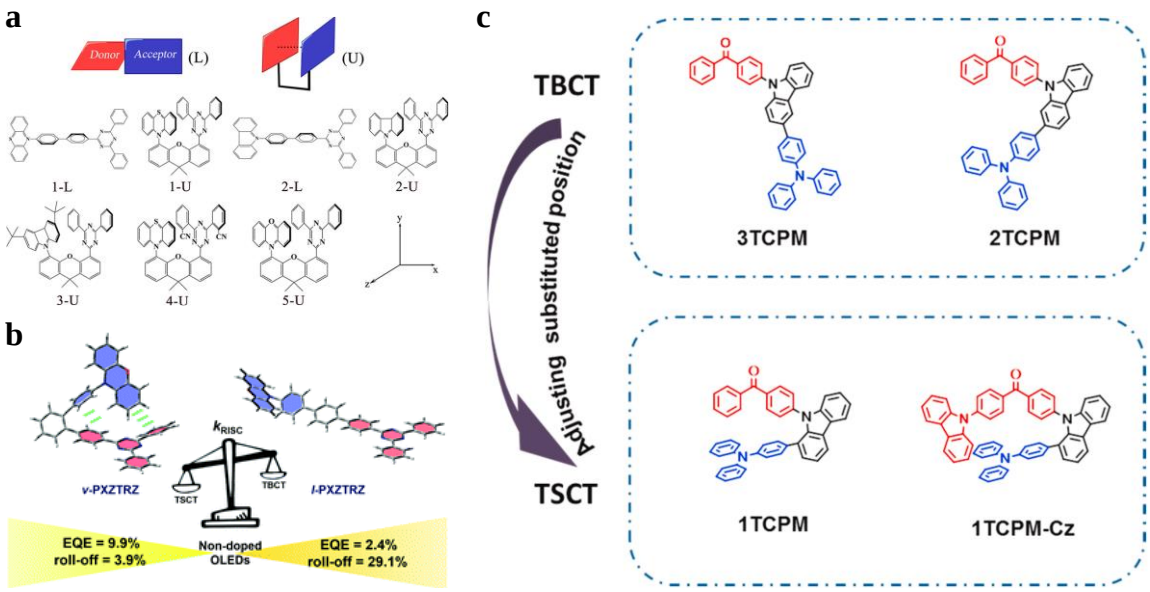

Figure 6. (a) Molecular structures of 1-L∼5-U; conventional conjugated D–A (L shape) and U-shaped space-through architecture (U shape) from ref.[45] (b) The comparison of external quantum efficiency (EQE) and efficiency roll-off between v-PXZTRZ and l-PXZTRZ from ref.[23] (c) Molecular structures and design strategy of the targeted TADF

emitters 1TCPM and 1TCPM-Cz from ref.[24] Copyright 2018, wiley; Copyright 2021, Elsevier; Copyright 2021, Royal Society of Chemistry.

2.3 Single-Molecule Junctions

Single-molecule-level electronic devices, also known as single-molecule junctions, have very significant importance in exceeding the intrinsic limitations of silicon-based electronic devices. The rational design of robust molecular wires capable of constructing reliable single-molecule junctions is fundamental to molecular electronics.[47, 48] Inspired by nature's efficient utilization of π-π stacking for directed long-range electron transport, it is believed that synthetic molecular wires incorporating π-π stacking will be available for use as new electronic materials or as components of molecular devices.[49, 50]

The artificial single-molecule can be broadly categorized into two main groups based on completely different modes of affixation: (1) rod-like molecules by TBCT, such as fully conjugated oligo(phenylene vinylidenes) (OPVs),[51] and (2) *para*-cyclophanes representing TSC between benzene rings with π-stacking.[52-54] Breslow *et al.* in 2011 were able to experimentally determine, for the first time, the single-molecule conductance of a synthetic molecular line with multiple tightly π-π stacking aromatic rings as shown in **Figure 7a**.[54] A new family of folders consisting of an increasing number of anthracene units that fold through a combination of intramolecular hydrogen bonding and aromatic interactions was reported by Alonso *et al.* in 2017.[55] As shown in **Figure 7b**, this folding process opened an efficient TSCT channel on the interacting anthracene part. The ultraviolet-visible electronic

spectra showed typical features of anthracene derivatives with four vibrational bands on the major electronic absorption in **Figure 7c (left)**. The electronic interactions between the anthracene parts could be observed since the absorption bands appeared increasingly red-shifted along with the increasing number of anthracene units in the oligomer. Intramolecular aromatic interactions between anthracenes were also evidenced by ultraviolet-visible PL studies in **Figure 7c (right)**. The presence of the anthracene excimer in the PL spectra evidenced the existence of a face-to-face overlap phenomenon between anthracenes in solution.

Up till now, experimental studies of intramolecular charge transport in molecular materials and electronic devices have been limited to conjugated systems involving π-π stacking interactions. Hong and Yang *et al.*[56] demonstrated that σ-σ stacking interactions between neighboring nonconjugated molecules provided an efficient pathway for charge transport through supramolecular junctions. The conductance of σ-σ stacked molecular junctions formed between two non-conjugated molecules was comparable to that of π-π stacked molecular junctions formed between π-conjugated benzene rings and exhibited TSCT properties (**Figure 7d**).

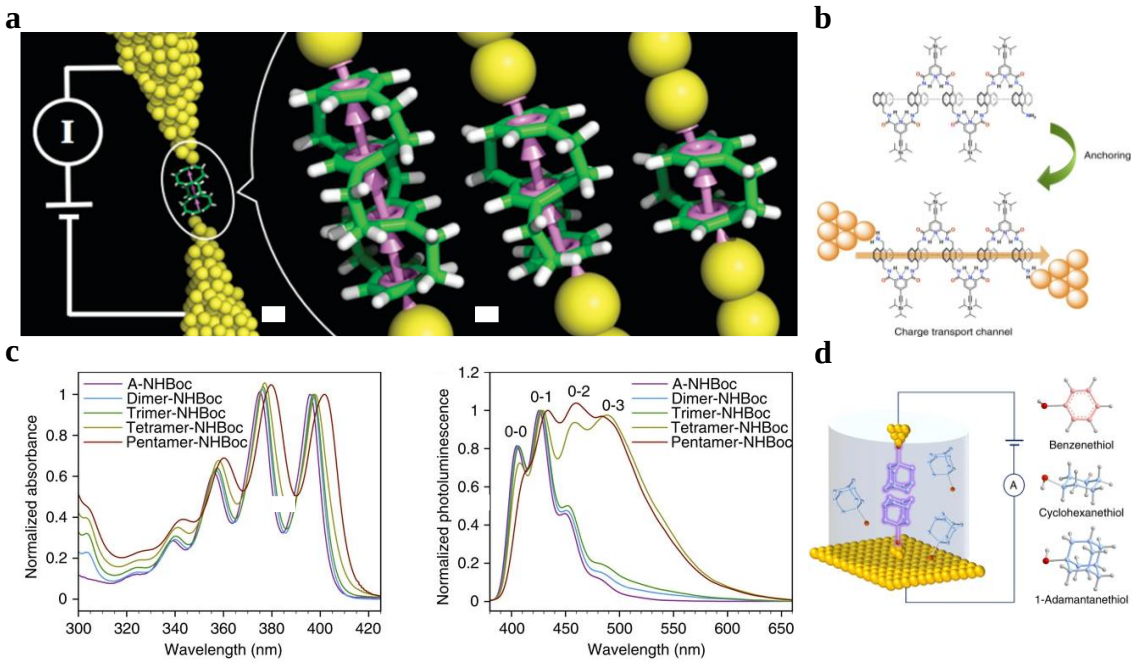

Figure 7. (a) Molecular wires with up to four π–π-stacked benzene rings from ref.[54] (b) Schematic representation of the folding and anchoring processes needed to obtain π-folded molecular junctions from a representative member of the foldamer family from ref.[55] (c) Absorption (left) and PL (right) spectra of the NHBoc foldamer series at 25 °C from ref.[55] (d) Break junction measurements of π-conjugated benzenethiol and non-conjugated cyclohexanethiol from ref.[56] Copyright 2011, American Chemical Society, Copyright 2017 2022, Nature.

Many of the single-molecule junctions in the literature were single-channel conductors realized by bonded or spatially conjugated molecules. However, due to the lack of powerful molecular wires, materials that have complementary multiple conductive channels that can enhance the conductivity and stability of molecular devices are very rare. A series of studies

on multichannel single-molecule wires have been carried out by Tang and Zhao *et al.* Two folded molecules were designed and synthesized with intramolecular π-π stacking interactions between a pair of biphenyls in 2015,[57] which were used for constructing single-molecule junctions with the simultaneous presence of two conductive channels in one junction (**Figure 8a**). Due to the insufficient contribution of spatial conduction channels, folded single-molecule wires only provided conductance similar to their conventional linear counterparts. Therefore, they proposed novel single-molecule wires based on hexaphenylbenzene (HPB) with typical TSCT structures in 2018 (**Figure 8b**).[58] The strong toroidal TSCT formed between the ring face-to-face aligned phenyls was significant and compensated for the excessive conductance loss of the weakened TBCT. Multichannel conductivity modeling by integrating space and bond conjugation may be a promising strategy for further design of robust single-molecule wires with advanced conductivity and stability.

In 2020, Tang and Zhao *et al* developed novel folded molecules with two parallel-aligned aryl chains,[59] in which the TSCT resulting from effective π-π interactions between the aryl chains could act as a complementary conduction channel to compensate for the loss of conductance when the TBCT channel was poor. They also presented a novel TSCT single-molecule parallel circuit (*f*-4Ph-4SMe) comprised of a pair of closely parallelly aligned *p*-quaterphenyl chains tethered by a vinyl bridge and end-capped with four SMe anchoring groups. As shown in **Figure 8c**, when four SMe groups were in contact with two electrodes at the same time, the through-bond and through-space conduction channels worked in

concert to produce a conductance, which was much larger than that of a similar molecule with two SMe groups or the sum of two *p*-quaterphenyl chains. This system was an ideal model for understanding electron transport through parallel π-stacked molecular systems and could serve as a key component of integrated molecular circuits with controllable conductance.

The single-molecular potentiometer based on *ortho*-pentaphenylene was further developed in 2021.[60] The *ortho*-pentaphenylene derivatives that were orthogonal and with anchoring groups adopted a multiple folded conformation and underwent conformational interchanges in solution. Solvent-sensitive multiple conductances originating from different conformational isomers were recorded by scanning tunneling microscopy break junction techniques. Tang and his colleagues designed single-molecule potentiometers based on *ortho*-pentaphenylene (**Figure 8d**).[60] The *ortho*-pentaphenylene derivatives with anchoring groups adopt multiple folded conformers and undergo conformational interconversion in solutions. Solvent-sensitive multiple conductance originating from different conformers is recorded by scanning tunneling microscopy break junction technique. These pseudo-elastic folded molecules can be stretched and compressed by mechanical force along with a variable conductance by up to two orders of magnitude, providing an impressively higher switching factor (114) than the reported values (ca. 1~25). These findings contributed to the exploration of robust single-molecule potentiometers based on helical structures and to the fundamental understanding of charge transport in higher-order helical molecules.

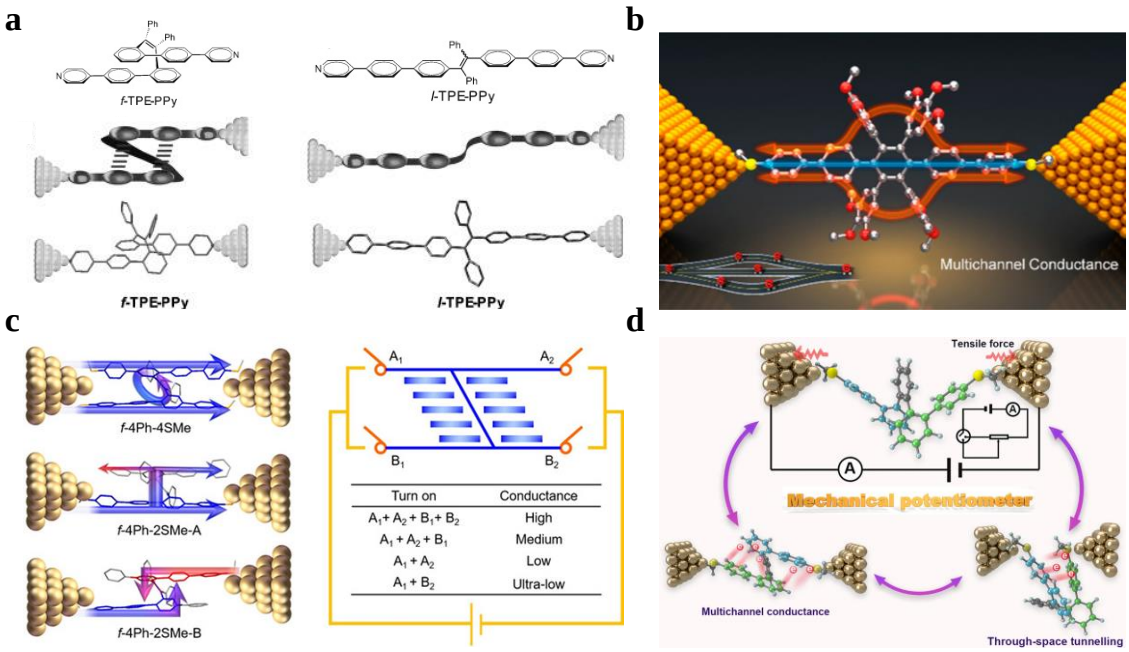

Figure 8. (a) Chemical structures and representation of circuits of *f*-TPE-PPy and *l*-TPE-PPy anchored onto gold electrodes from ref.[57] (b) Schematic representation of circuits of HPB(OM)$_3$-SM anchored onto gold electrodes from ref.[58] (c) The electron-transport mechanism in *f*-4Ph-4SMe, *f*-4Ph-2SMe-A, and *f*-4Ph-2SMe-B. A controllable multichannel-molecular-device model was depicted based on the single-molecule parallel circuit *f*-4Ph-4SMe from ref.[59] (d) Schematic illustration of a mechanical single-molecule potentiometer based on *o*-PP-2SMe from ref.[60] Copyright 2015 2020, wiley; Copyright 2018, American Chemical Society; Copyright 2021, nature.

2.4 Photoswitches

TSCT shows the advantages of flexibility and tunability in multidimensional charge transport. Therefore, it has become a hot research area for optical drive applications. The donors and acceptors in most molecules are usually locked in coplanar configurations,

resulting in charge recombination that destroys the energy conversion efficiency. On the contrary, configuration change will help to regulate the charge dynamics at the excited state to ensure charge separation. The charge transfer process can be efficiently induced by changing the molecular configuration in a specified manner.[61-63] Photoswitches, which can undergo significant geometrical configuration changes upon light-induced isomerization and provide a non-contact way of adjusting the molecular structure, can serve as ideal dynamic linkers.[64-66] Zhang and He *et al.*[67] chose bridged azobenzene (BAB) as the photoswitch, which was exactly suitable for dynamic control of the TSCT process. At the ground state, it prefers the compact *Z* isomer to the extended *E* isomer. As shown in **Figure 9b**, *Z* isomer will turn to *E* isomer upon exposure of blue light (370–400 nm); and *E* switches back to *Z* in the condition of green light (480–550 nm) irradiation.[68] They developed a donor-switch-acceptor (DSA) model with a framework similar to the reported donor-linker-acceptor molecular system,[5, 11] which worked by TSCT. However, the structure of the switch is sensitive and adaptive according to the light. To make TSCT occur in the DSA molecule, the frontier orbital energy levels of each unit (i.e., D, S, and A) need to follow a specific arrangement. As shown in **Figure 9a**, the highest occupied molecular orbital (HOMO) energy levels of D, S, and A were decreasing in order, and the lowest unoccupied molecular orbital (LUMO) energy levels were, in the descending order of S>D>A. In this case, the electrons would be excited from their HOMO (corresponding to donor units) and transferred to the LUMO (corresponding to donor units) rather than to S. The structure of donors and acceptors, and the energy levels of frontier orbitals of selected

donor, switch, and acceptors were also collected in **Figure 9a**. The *Z* isomer of BAB facilitated π-π stacking of D-A pairs with a specified arrangement of frontier orbitals to ensure TSCT, whereas the *E* isomer of BAB disrupted this stacking and inhibited charge recombination. It demonstrated the potential of using specific photoswitches within stacked π systems for photochemical conversion.

The most common method for realizing single-molecule photoswitches is photo-induced switching.[69-72] The switching process can be induced by irradiation to induce changes such as photoisomerization,[73] intramolecular energy transfer,[74], and intersystem crossing to the triplet state.[75] The application of external electric field (EF)/potential could also be used to modulate the photon emission properties of molecular systems. Different from photoinduced switching, the application of EF in the integrated design of functional single-molecule switches may be more convenient because EFs are available in biased metal nano-junctions. Luo and Tian *et al.*[76] proposed a new mechanism using in single-molecule photoswitch. The EF in a biased metal nano-junction controlled emission from molecules with TSCT excited states. The EF-induced Stark effect was able to flip the order of the bright non-charge transfer state and the dark TSCT state, resulting in the desired switching behavior. A schematic picture of the considered model system and the optimized geometry of the NDIC-Ome molecule are depicted in **Figure 9c**. The molecule was placed in a nanocavity formed by the STM tip and substrate, with the bottom NDI chromophore attached in parallel to the substrate. Owing to the weak coupling limitation, the electron tunneling process could be described by sequential tunneling (SET). If it was assumed that

the tunneling process was triggered by an electron penetrating out of the occupied molecular orbital tunnel to the substrate, the tunneling-induced molecular lepton and photon emission processes could be described by the minimal three-state model[77] (**Figure 9c**), where the green and red arrows represent the charge transport and photon emission processes, respectively. According to the strength of the applied field, the EL process involved three excited states, i.e., two TSCT states, CT*m* and CT*p*, and one non-CT state *n*CT. The charge transfer characteristics of the two TSCT states can be identified clearly. Due to the small overlap between the molecular orbitals involved, the oscillation strengths of both TSCT states were much smaller than those of the non-CT state. Without considering the EF effect, the EL energy (3.22 eV) and intensity were the same under both EFs, as in **Figure 9d**. The EL spectra were the same under -4.114 V, with or without considering the effect of EF. These results indicated that *in situ* EF in single-molecule junctions could play an important role in the optical properties of the molecules and facilitate the design of single-molecule optoelectronic devices.

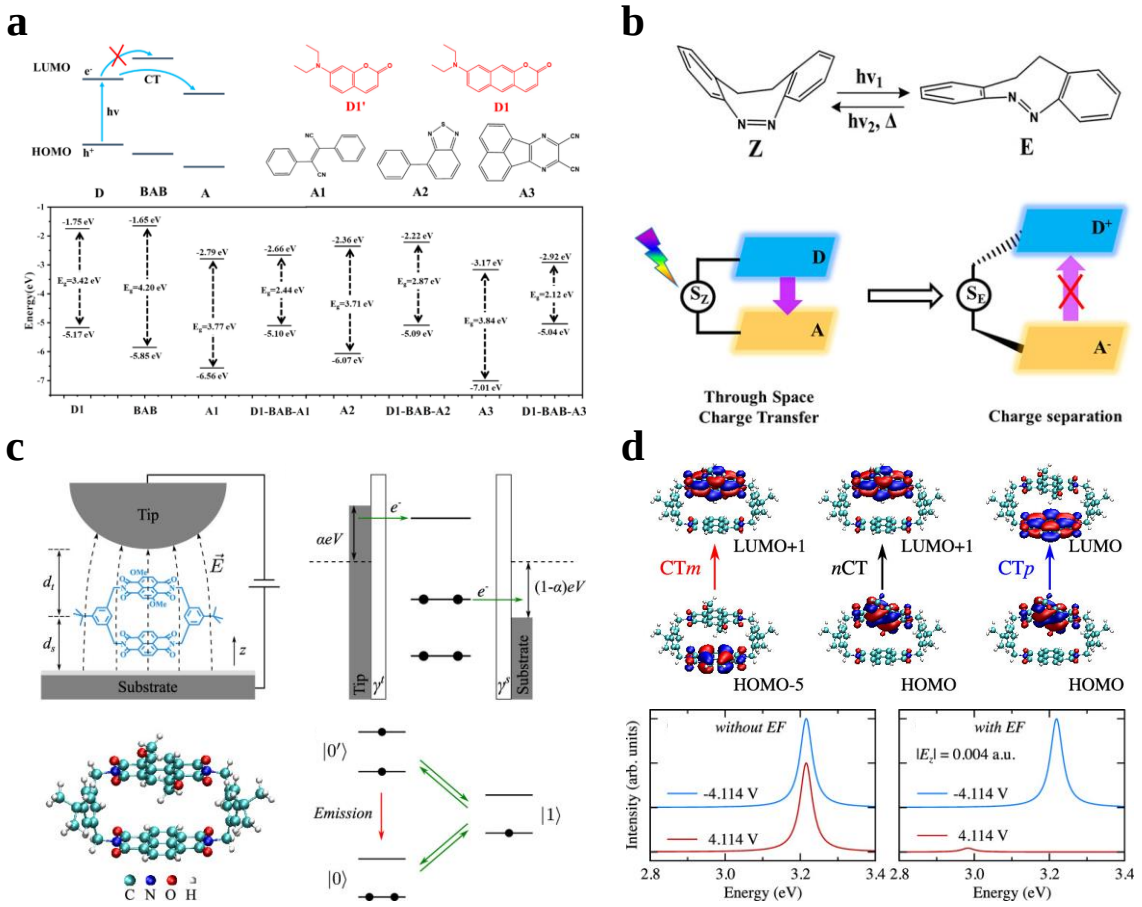

Figure 9. (a) Fragmental frontier molecular orbital energy level diagram in D-S-A for TSCT; the structural formula of selected electron donors and acceptors; HOMO–LUMO gap diagrams for chosen donor, switch, and acceptors and three D-S-A complexes from ref.[67] (b) BAB enables TSCT via E/Z isomerization from ref.[67] (c) Schematic drawing of the setup for the investigated STM-EL measurement with the NDIC-OMe molecule under the *in situ* electric field; optimized geometry of the NDIC-OMe molecule; energetic diagram for the electron tunneling process in the sequential tunneling regime; model describing the tunneling-induced electronic state transitions and the photon emission process from ref.[76] (d) Major molecular orbital transitions for the three excited states that are involved in the photon emission process; bias polarity dependent EL of the NDIC-OMe

molecule from ref.[76] Copyright 2021, American Chemical Society.

3. Outlook and Perspectives

As one of the most important ways of electron interaction, TSI is characterized by non-covalent bonding between overlapping aromatic rings at a close distance. Owing to its unique flexibility and tunability in multidimensional charge transport, it has various attractive advantages in organic optoelectronic devices.

The development of high-performance OFFSs based on TSCT is a promising area of research due to unique molecular structural features. The precisely controlled distance and face-to-face alignment between the donor and acceptor would not only create abundant gaps in the adlayer of the film, but also provide a space to accommodate VOCs. However, organic fluorophores are very scarce for ultrasensitive alkane sensing. Considering the volatility and chemical inertness of alkanes, further exploration of various TSCT-based sensing fluorophores is challenging but rewarding. Innovative molecular design and optimization of adlayer structure are expected to further promote the development of high-performance OFFSs.

For OLED, highly twisted molecular TSCT structures can increase spatial conjugation and enrich intramolecular interactions. This can reduce the overlapping between HOMO and LUMO, realizing small ΔE_{ST} values. Moreover, the steric hindrance caused by twisted molecules can reduce the vibration and rotation of molecules, thus reducing non-radiative decay and improving the utilization of triplet excitons. Intramolecular noncovalent

interactions between the donor and acceptor further suppress the nonradiative decay, avoiding the dropping of quantum yield caused by intermolecular π-π interactions in the solid state and improving the device performance by reducing the efficiency roll-off.

In terms of single-molecule wires, long-range electron transport depends not only on the chemical structure of individual molecules and the intrinsic properties due to π-stacking, but also on the spatial structure of these molecules. Enhanced spatial interactions will expand the jump dipole moment and spin-orbit coupling, which will further accelerate the upconversion process and create additional charge transfer channels. The strong toroidal TSI formed between the face-to-face groups is significant and compensates for the excessive conductance loss of the weakened through-bond counterpart. Multichannel conductivity modeling by integrating space and bond conjugation may be a promising strategy for further design of robust, stable, and conductive single-molecule wires.

Regarding photoswitches, the selection of them as linkers between donors and acceptors in TSCT molecules can effectively direct charge transfer within π-stacking systems to realize the potential for photochemical conversion. Moreover, using the new mechanism of *in situ* photoswitch to bias the EF in the metal nanoconjunctions can control the photon emission from molecules with TSCT excited states. The EF-induced Stark effect can flip the order of the bright non-charge transfer state and the dark TSCT state, resulting in the desired switching behavior. These results indicate that the molecular structure with TSI plays an important role in the optical properties of the photoswitches and facilitates the design of organic optoelectronic devices.

ACKNOWLEDGEMENTS

The authors thank the financial support from the National Natural Science Foundation of China (52303382), Guangdong Basic and Applied Basic Research Foundation (2023A1515011342), Shenzhen Key Laboratory of Functional Aggregate Materials (ZDSYS20211021111400001), and the Science, Technology and Innovation Commission of Shenzhen Municipality (KQTD20210811090142053, JCYJ20220530143805012).

Reference

1. Burroughes, J. H.; Bradley, D. D. C.; Brown, A. R.; Marks, R. N.; Mackay, K.; Friend, R. H.; Burns, P. L.; Holmes, A. B. Light-emitting diodes based on conjugated polymers. *Nature* **1990**, *347* (6293), 539-541. DOI: 10.1038/347539a0.
2. Baldo, M. A.; O'Brien, D. F.; You, Y.; Shoustikov, A.; Sibley, S.; Thompson, M. E.; Forrest, S. R. Highly efficient phosphorescent emission from organic electroluminescent devices. *Nature* **1998**, *395* (6698), 151-154. DOI: 10.1038/25954.
3. Sun, Y.; Giebink, N. C.; Kanno, H.; Ma, B.; Thompson, M. E.; Forrest, S. R. Management of singlet and triplet excitons for efficient white organic light-emitting devices. *Nature* **2006**, *440* (7086), 908-912. DOI: 10.1038/nature04645.
4. Reineke, S.; Lindner, F.; Schwartz, G.; Seidler, N.; Walzer, K.; Lüssem, B.; Leo, K. White organic light-emitting diodes with fluorescent tube efficiency. *Nature* **2009**, *459* (7244), 234-238. DOI: 10.1038/nature08003.
5. Uoyama, H.; Goushi, K.; Shizu, K.; Nomura, H.; Adachi, C. Highly efficient organic light-emitting diodes from delayed fluorescence. *Nature* **2012**, *492* (7428), 234-238. DOI: 10.1038/nature11687.
6. Li, H.; Shi, W.; Song, J.; Jang, H.-J.; Dailey, J.; Yu, J.; Katz, H. E. Chemical and Biomolecule Sensing with Organic Field-Effect Transistors. *Chem. Rev.* **2019**, *119* (1), 3-35. DOI: 10.1021/acs.chemrev.8b00016.
7. Xu, Y.; Sun, H.; Liu, A.; Zhu, H.-H.; Li, W.; Lin, Y.-F.; Noh, Y.-Y. Doping: A Key Enabler for Organic Transistors. *Adv. Mater.* **2018**, *30* (46), 1801830. DOI: https://doi.org/10.1002/adma.201801830 (acccessed 2023/09/22).
8. Huo, Y.; Zhang, H.-L.; Zhan, X. Nonfullerene All-Small-Molecule Organic Solar Cells. *ACS Energy Lett.* **2019**, *4* (6), 1241-1250. DOI: 10.1021/acsenergylett.9b00528.
9. Wada, Y.; Nakagawa, H.; Matsumoto, S.; Wakisaka, Y.; Kaji, H. Organic light emitters exhibiting very fast reverse intersystem crossing. *Nat. Photonics* **2020**, *14* (10), 643-649. DOI: 10.1038/s41566-020-0667-0.

10. Yang, S.-Y.; Qu, Y.-K.; Liao, L.-S.; Jiang, Z.-Q.; Lee, S.-T. Research Progress of Intramolecular π-Stacked Small Molecules for Device Applications. *Adv. Mater.* **2022**, *34* (22), 2104125. DOI: https://doi.org/10.1002/adma.202104125 (acccessed 2023/09/20).
11. Tsujimoto, H.; Ha, D.-G.; Markopoulos, G.; Chae, H. S.; Baldo, M. A.; Swager, T. M. Thermally Activated Delayed Fluorescence and Aggregation Induced Emission with Through-Space Charge Transfer. *J. Am. Chem. Soc.* **2017**, *139* (13), 4894-4900. DOI: 10.1021/jacs.7b00873.
12. Wu, C.; Liu, W.; Li, K.; Cheng, G.; Xiong, J.; Teng, T.; Che, C.-M.; Yang, C. Face-to-Face Orientation of Quasiplanar Donor and Acceptor Enables Highly Efficient Intramolecular Exciplex Fluorescence. *Angew. Chem. Int. Ed.* **2021**, *60* (8), 3994-3998. DOI: https://doi.org/10.1002/anie.202013051 (acccessed 2023/09/20).
13. Liu, C.; Xiao, F.; Li, Y.; Lei, D.; Liu, Y.; Ma, X.; Gu, C.; Dou, X. Intermolecular through-space charge transfer enabled by bicomponent assembly for ultrasensitive detection of synthetic cannabinoid JWH-018. *Aggregate* **2023**, *4* (4), e315. DOI: https://doi.org/10.1002/agt2.315 (acccessed 2023/10/08).
14. Zheng, Q.; Wang, X.-Q.; Qu, Y.-K.; Xie, G.; Liao, L.-S.; Jiang, Z.-Q. Solution-processable through-space charge-transfer emitters via solubilizing groups modification. *npj Flex. Electron.* **2022**, *6* (1), 83. DOI: 10.1038/s41528-022-00212-5.
15. Shao, S.; Wang, L. Through-space charge transfer polymers for solution-processed organic light-emitting diodes. *Aggregate* **2020**, *1* (1), 45-56. DOI: https://doi.org/10.1002/agt2.4 (acccessed 2023/10/08).
16. Liu, J.; Zhang, H.; Hu, L.; Wang, J.; Lam, J. W. Y.; Blancafort, L.; Tang, B. Z. Through-Space Interaction of Tetraphenylethylene: What, Where, and How. *J. Am. Chem. Soc.* **2022**, *144* (17), 7901-7910. DOI: 10.1021/jacs.2c02381.
17. Zhao, Z.; Zhang, H.; Lam, J. W. Y.; Tang, B. Z. Aggregation-Induced Emission: New Vistas at the Aggregate Level. *Angew. Chem. Int. Ed.* **2020**, *59* (25), 9888-9907. DOI: https://doi.org/10.1002/anie.201916729 (acccessed 2023/10/13).
18. Zhang, H.; Zheng, X.; Xie, N.; He, Z.; Liu, J.; Leung, N. L. C.; Niu, Y.; Huang, X.; Wong, K. S.; Kwok, R. T. K.; et al. Why Do Simple Molecules with "Isolated" Phenyl Rings Emit Visible Light? *J. Am. Chem. Soc.* **2017**, *139* (45), 16264-16272. DOI: 10.1021/jacs.7b08592.
19. Sturala, J.; Etherington, M. K.; Bismillah, A. N.; Higginbotham, H. F.; Trewby, W.; Aguilar, J. A.; Bromley, E. H. C.; Avestro, A.-J.; Monkman, A. P.; McGonigal, P. R. Excited-State Aromatic Interactions in the Aggregation-Induced Emission of Molecular Rotors. *J. Am. Chem. Soc.* **2017**, *139* (49), 17882-17889. DOI: 10.1021/jacs.7b08570.
20. Xiong, Z.; Zhang, J.; Wang, L.; Xie, Y.; Wang, Y.; Zhao, Z.; Zhang, H.; Zhi Sun, J.; Huang, F.; Tang Ben, Z. Controllable Secondary Through-Space Interaction and Clusteroluminescence. *CCS Chemistry* **2023**, *0* (0), 1-13. DOI: 10.31635/ccschem.023.202302815 (acccessed 2023/10/13).
21. Zhang, Z.; Zhang, J.; Xiong, Z.; Chu, B.; Zhang, C.; Sun, J. Z.; Zhang, H.; Zhang, X.-H.; Tang, B. Z. NIR Clusteroluminescence of Non-conjugated Phenolic Resins Enabled by

Through-Space Interactions. *Angew. Chem. Int. Ed.* **2023**, *62* (30), e202306762. DOI: https://doi.org/10.1002/anie.202306762 (acccessed 2023/10/13).
22. Zhang, J.; Alam, P.; Zhang, S.; Shen, H.; Hu, L.; Sung, H. H. Y.; Williams, I. D.; Sun, J.; Lam, J. W. Y.; Zhang, H.; et al. Secondary through-space interactions facilitated single-molecule white-light emission from clusteroluminogens. *Nat. Commun.* **2022**, *13* (1), 3492. DOI: 10.1038/s41467-022-31184-9.
23. Yu, M.; Zhu, X.; Zeng, J.; Liu, H.; Huang, R.; Zhuang, Z.; Shen, P.; Zhao, Z.; Tang, B. Z. Comparative study on the impact of through-space charge transfer over the electroluminescence performance of delayed fluorescence molecules. *J. Mater. Chem. C* **2021**, *9* (41), 14808-14814, 10.1039/D1TC03564A. DOI: 10.1039/D1TC03564A.
24. Ma, F.; Ji, H.; Zhang, D.; Xue, K.; Zhang, P.; Qi, Z.; Zhu, H. Adjusting the photophysical properties of AIE-active TADF emitters from through-bond to through-space charge transfer for high-performance solution-processed OLEDs. *Dyes Pigm.* **2021**, *188*, 109208. DOI: https://doi.org/10.1016/j.dyepig.2021.109208.
25. Brédas, J.-L.; Beljonne, D.; Coropceanu, V.; Cornil, J. Charge-Transfer and Energy-Transfer Processes in π-Conjugated Oligomers and Polymers: A Molecular Picture. *Chem. Rev.* **2004**, *104* (11), 4971-5004. DOI: 10.1021/cr040084k.
26. Pace, C. J.; Gao, J. Exploring and Exploiting Polar−π Interactions with Fluorinated Aromatic Amino Acids. *Acc. Chem. Res.* **2013**, *46* (4), 907-915. DOI: 10.1021/ar300086n.
27. Wang, Z.; Gou, X.; Shi, Q.; Liu, K.; Chang, X.; Wang, G.; Xu, W.; Lin, S.; Liu, T.; Fang, Y. Through-Space Charge Transfer: A New Way to Develop a High-Performance Fluorescence Sensing Film towards Opto-Electronically Inert Alkanes. *Angew. Chem. Int. Ed.* **2022**, *61* (35), e202207619. DOI: https://doi.org/10.1002/anie.202207619 (acccessed 2023/10/14).
28. Yang, Z.; Mao, Z.; Xie, Z.; Zhang, Y.; Liu, S.; Zhao, J.; Xu, J.; Chi, Z.; Aldred, M. P. Recent advances in organic thermally activated delayed fluorescence materials. *Chem. Soc. Rev.* **2017**, *46* (3), 915-1016, 10.1039/C6CS00368K. DOI: 10.1039/C6CS00368K.
29. Liu, Y.; Li, C.; Ren, Z.; Yan, S.; Bryce, M. R. All-organic thermally activated delayed fluorescence materials for organic light-emitting diodes. *Nat. Rev. Mater.* **2018**, *3* (4), 18020. DOI: 10.1038/natrevmats.2018.20.
30. Data, P.; Takeda, Y. Recent Advancements in and the Future of Organic Emitters: TADF- and RTP-Active Multifunctional Organic Materials. *Chem. Asian J* **2019**, *14* (10), 1613-1636. DOI: https://doi.org/10.1002/asia.201801791 (acccessed 2023/09/22).
31. Zhang, W.; Kong, J.; An, R. Z.; Zhang, J.; Zhou, Y.; Cui, L.-S.; Zhou, M. Engineering singlet and triplet excitons of TADF emitters by different host-guest interactions. *Aggregate* **2023**, *n/a* (n/a), e416. DOI: https://doi.org/10.1002/agt2.416 (acccessed 2023/10/08).
32. Alam, M. I.; Nagar, M. R.; Nayak, S. R.; Choudhury, A.; Jou, J.-H.; Vaidyanathan, S. Acceptor Interlocked Molecular Design for Solution-Processed Stable Deep-Blue TADF and Hyper Fluorescence Organic LED Enabling High-Efficiency. *Adv. Opt. Mater.* **2022**, *10* (18), 2200376. DOI: https://doi.org/10.1002/adom.202200376 (acccessed 2023/09/22).

33. Lee, Y.-T.; Chan, C.-Y.; Tanaka, M.; Mamada, M.; Balijapalli, U.; Tsuchiya, Y.; Nakanotani, H.; Hatakeyama, T.; Adachi, C. Investigating HOMO Energy Levels of Terminal Emitters for Realizing High-Brightness and Stable TADF-Assisted Fluorescence Organic Light-Emitting Diodes. *Adv. Electron. Mater.* **2021**, *7* (4), 2001090. DOI: https://doi.org/10.1002/aelm.202001090 (acccessed 2023/09/22).
34. Braveenth, R.; Lee, H.; Park, J. D.; Yang, K. J.; Hwang, S. J.; Naveen, K. R.; Lampande, R.; Kwon, J. H. Achieving Narrow FWHM and High EQE Over 38% in Blue OLEDs Using Rigid Heteroatom-Based Deep Blue TADF Sensitized Host. *Adv. Funct. Mater.* **2021**, *31* (47), 2105805. DOI: https://doi.org/10.1002/adfm.202105805 (acccessed 2023/09/22).
35. Lim, H.; Cheon, H. J.; Woo, S.-J.; Kwon, S.-K.; Kim, Y.-H.; Kim, J.-J. Highly Efficient Deep-Blue OLEDs using a TADF Emitter with a Narrow Emission Spectrum and High Horizontal Emitting Dipole Ratio. *Adv. Mater.* **2020**, *32* (47), 2004083. DOI: https://doi.org/10.1002/adma.202004083 (acccessed 2023/09/22).
36. Cheng, H. F.; Johnson, J. A. Controlling the orientation of hole transport molecules in bottlebrush polymers for enhanced OLED performance. *Aggregate* **2022**, *3* (5), e259. DOI: https://doi.org/10.1002/agt2.259 (acccessed 2023/10/08).
37. Zhang, J.; Wei, Q.; Li, W.; Chen, H.; Zhu, X.; Bai, Y.; Fei, N.; Cao, L.; Zhao, Z.; Qin, A.; et al. AIEgen configuration transition and aggregation enable dual prompt emission for single-component nondoped white OLEDs. *Aggregate* **2023**, *n/a* (n/a), e410. DOI: https://doi.org/10.1002/agt2.410 (acccessed 2023/10/08).
38. Xue, Q.; Xie, G. Thermally Activated Delayed Fluorescence beyond Through-Bond Charge Transfer for High-Performance OLEDs. *Adv. Opt. Mater.* **2021**, *9* (14), 2002204. DOI: https://doi.org/10.1002/adom.202002204 (acccessed 2023/09/22).
39. Bui, T.-T.; Goubard, F.; Ibrahim-Ouali, M.; Gigmes, D.; Dumur, F. Recent advances on organic blue thermally activated delayed fluorescence (TADF) emitters for organic light-emitting diodes (OLEDs). *Beilstein J. Org. Chem.* **2018**, *14*, 282-308. DOI: 10.3762/bjoc.14.18.
40. Yang, Z.; Mao, Z.; Xu, C.; Chen, X.; Zhao, J.; Yang, Z.; Zhang, Y.; Wu, W.; Jiao, S.; Liu, Y.; et al. A sterically hindered asymmetric D–A–D′ thermally activated delayed fluorescence emitter for highly efficient non-doped organic light-emitting diodes. *Chem. Sci.* **2019**, *10* (35), 8129-8134, 10.1039/C9SC01686D. DOI: 10.1039/C9SC01686D.
41. Lin, T.-C.; Sarma, M.; Chen, Y.-T.; Liu, S.-H.; Lin, K.-T.; Chiang, P.-Y.; Chuang, W.-T.; Liu, Y.-C.; Hsu, H.-F.; Hung, W.-Y.; et al. Probe exciplex structure of highly efficient thermally activated delayed fluorescence organic light emitting diodes. *Nat. Commun.* **2018**, *9* (1), 3111. DOI: 10.1038/s41467-018-05527-4.
42. Tang, X.; Cui, L.-S.; Li, H.-C.; Gillett, A. J.; Auras, F.; Qu, Y.-K.; Zhong, C.; Jones, S. T. E.; Jiang, Z.-Q.; Friend, R. H.; et al. Highly efficient luminescence from space-confined charge-transfer emitters. *Nat. Mater.* **2020**, *19* (12), 1332-1338. DOI: 10.1038/s41563-020-0710-z.
43. Wang, X.-Q.; Yang, S.-Y.; Tian, Q.-S.; Zhong, C.; Qu, Y.-K.; Yu, Y.-J.; Jiang, Z.-Q.; Liao, L.-S. Multi-Layer π-Stacked Molecules as Efficient Thermally Activated Delayed

Fluorescence Emitters. *Angew. Chem. Int. Ed.* **2021**, *60* (10), 5213-5219. DOI: https://doi.org/10.1002/anie.202011384 (acccessed 2023/09/21).
44. Xie, F.-M.; Li, H.-Z.; Zhang, K.; Shen, Y.; Zhao, X.; Li, Y.-Q.; Tang, J.-X. A Dislocated Twin-Locking Acceptor-Donor-Acceptor Configuration for Efficient Delayed Fluorescence with Multiple Through-Space Charge Transfer. *Angew. Chem. Int. Ed.* **2022**, *61* (49), e202213823. DOI: https://doi.org/10.1002/anie.202213823 (acccessed 2023/09/21).
45. Ye, J.-T.; Wang, L.; Wang, H.-Q.; Pan, X.-M.; Xie, H.-M.; Qiu, Y.-Q. Effective Impact of Dielectric Constant on Thermally Activated Delayed Fluorescence and Nonlinear Optical Properties: Through-Bond/-Space Charge Transfer Architectures. *J. Phys. Chem. C* **2018**, *122* (33), 18850-18859. DOI: 10.1021/acs.jpcc.8b05411.
46. Peng, C.-C.; Yang, S.-Y.; Li, H.-C.; Xie, G.-H.; Cui, L.-S.; Zou, S.-N.; Poriel, C.; Jiang, Z.-Q.; Liao, L.-S. Highly Efficient Thermally Activated Delayed Fluorescence via an Unconjugated Donor–Acceptor System Realizing EQE of Over 30%. *Adv. Mater.* **2020**, *32* (48), 2003885. DOI: https://doi.org/10.1002/adma.202003885 (acccessed 2023/09/22).
47. Nitzan, A.; Ratner, M. A. Electron Transport in Molecular Wire Junctions. *Science* **2003**, *300* (5624), 1384-1389. DOI: 10.1126/science.1081572 (acccessed 2023/09/21).
48. Tao, N. J. Electron transport in molecular junctions. *Nat. Nanotechnol.* **2006**, *1* (3), 173-181. DOI: 10.1038/nnano.2006.130.
49. Wu, W.; Liu, Y.; Zhu, D. π-Conjugated molecules with fused rings for organic field-effect transistors: design, synthesis and applications. *Chem. Soc. Rev.* **2010**, *39* (5), 1489-1502, 10.1039/B813123F. DOI: 10.1039/B813123F.
50. Solomon, G. C.; Herrmann, C.; Vura-Weis, J.; Wasielewski, M. R.; Ratner, M. A. The Chameleonic Nature of Electron Transport through π-Stacked Systems. *J. Am. Chem. Soc.* **2010**, *132* (23), 7887-7889. DOI: 10.1021/ja102434m.
51. Sikes, H. D.; Smalley, J. F.; Dudek, S. P.; Cook, A. R.; Newton, M. D.; Chidsey, C. E. D.; Feldberg, S. W. Rapid Electron Tunneling Through Oligophenylenevinylene Bridges. *Science* **2001**, *291* (5508), 1519-1523. DOI: 10.1126/science.1055745 (acccessed 2023/09/21).
52. Batra, A.; Kladnik, G.; Vázquez, H.; Meisner, J. S.; Floreano, L.; Nuckolls, C.; Cvetko, D.; Morgante, A.; Venkataraman, L. Quantifying through-space charge transfer dynamics in π-coupled molecular systems. *Nat. Commun.* **2012**, *3* (1), 1086. DOI: 10.1038/ncomms2083.
53. Seferos, D. S.; Blum, A. S.; Kushmerick, J. G.; Bazan, G. C. Single-Molecule Charge-Transport Measurements that Reveal Technique-Dependent Perturbations. *J. Am. Chem. Soc.* **2006**, *128* (34), 11260-11267. DOI: 10.1021/ja062898j.
54. Schneebeli, S. T.; Kamenetska, M.; Cheng, Z.; Skouta, R.; Friesner, R. A.; Venkataraman, L.; Breslow, R. Single-Molecule Conductance through Multiple π–π-Stacked Benzene Rings Determined with Direct Electrode-to-Benzene Ring Connections. *J. Am. Chem. Soc.* **2011**, *133* (7), 2136-2139. DOI: 10.1021/ja111320n.
55. Carini, M.; Ruiz, M. P.; Usabiaga, I.; Fernández, J. A.; Cocinero, E. J.; Melle-Franco,

M.; Diez-Perez, I.; Mateo-Alonso, A. High conductance values in π-folded molecular junctions. *Nat. Commun.* **2017**, *8* (1), 15195. DOI: 10.1038/ncomms15195.
56. Feng, A.; Zhou, Y.; Al-Shebami, M. A. Y.; Chen, L.; Pan, Z.; Xu, W.; Zhao, S.; Zeng, B.; Xiao, Z.; Yang, Y.; et al. σ–σ Stacked supramolecular junctions. *Nat. Chem.* **2022**, *14* (10), 1158-1164. DOI: 10.1038/s41557-022-01003-1.
57. Chen, L.; Wang, Y.-H.; He, B.; Nie, H.; Hu, R.; Huang, F.; Qin, A.; Zhou, X.-S.; Zhao, Z.; Tang, B. Z. Multichannel Conductance of Folded Single-Molecule Wires Aided by Through-Space Conjugation. *Angew. Chem. Int. Ed.* **2015**, *54* (14), 4231-4235. DOI: https://doi.org/10.1002/anie.201411909 (acccessed 2023/09/21).
58. Zhen, S.; Mao, J.-C.; Chen, L.; Ding, S.; Luo, W.; Zhou, X.-S.; Qin, A.; Zhao, Z.; Tang, B. Z. Remarkable Multichannel Conductance of Novel Single-Molecule Wires Built on Through-Space Conjugated Hexaphenylbenzene. *Nano Lett.* **2018**, *18* (7), 4200-4205. DOI: 10.1021/acs.nanolett.8b01082.
59. Shen, P.; Huang, M.; Qian, J.; Li, J.; Ding, S.; Zhou, X.-S.; Xu, B.; Zhao, Z.; Tang, B. Z. Achieving Efficient Multichannel Conductance in Through-Space Conjugated Single-Molecule Parallel Circuits. *Angew. Chem. Int. Ed.* **2020**, *59* (11), 4581-4588. DOI: https://doi.org/10.1002/anie.202000061 (acccessed 2023/09/21).
60. Li, J.; Shen, P.; Zhen, S.; Tang, C.; Ye, Y.; Zhou, D.; Hong, W.; Zhao, Z.; Tang, B. Z. Mechanical single-molecule potentiometers with large switching factors from ortho-pentaphenylene foldamers. *Nat. Commun.* **2021**, *12* (1), 167. DOI: 10.1038/s41467-020-20311-z.
61. Grabowski, Z. R.; Rotkiewicz, K.; Rettig, W. Structural Changes Accompanying Intramolecular Electron Transfer: Focus on Twisted Intramolecular Charge-Transfer States and Structures. *Chem. Rev.* **2003**, *103* (10), 3899-4032. DOI: 10.1021/cr9407451.
62. Thompson, A. L.; Ahn, T.-S.; Thomas, K. R. J.; Thayumanavan, S.; Martínez, T. J.; Bardeen, C. J. Using Meta Conjugation To Enhance Charge Separation versus Charge Recombination in Phenylacetylene Donor−Bridge−Acceptor Complexes. *J. Am. Chem. Soc.* **2005**, *127* (47), 16348-16349. DOI: 10.1021/ja054543q.
63. Cheng, Y.; Qi, Y.; Tang, Y.; Zheng, C.; Wan, Y.; Huang, W.; Chen, R. Controlling Intramolecular Conformation through Nonbonding Interaction for Soft-Conjugated Materials: Molecular Design and Optoelectronic Properties. *J. Phys. Chem. Lett.* **2016**, *7* (18), 3609-3615. DOI: 10.1021/acs.jpclett.6b01695.
64. Castellanos, S.; Vieira, A. A.; Illescas, B. M.; Sacchetti, V.; Schubert, C.; Moreno, J.; Guldi, D. M.; Hecht, S.; Martín, N. Gating Charge Recombination Rates through Dynamic Bridges in Tetrathiafulvalene–Fullerene Architectures. *Angew. Chem. Int. Ed.* **2013**, *52* (52), 13985-13990. DOI: https://doi.org/10.1002/anie.201306183 (acccessed 2023/09/21).
65. Russew, M.-M.; Hecht, S. Photoswitches: From Molecules to Materials. *Adv. Mater.* **2010**, *22* (31), 3348-3360. DOI: https://doi.org/10.1002/adma.200904102 (acccessed 2023/09/21).
66. Wu, Z.; Cui, P.; Zhang, G.; Luo, Y.; Jiang, J. Self-Adaptive Switch Enabling Complete Charge Separation in Molecular-Based Optoelectronic Conversion. *J. Phys. Chem. Lett.*

2018, *9* (4), 837-843. DOI: 10.1021/acs.jpclett.8b00119.
67. Zhou, H.; He, F.; Chong, Y.; He, L.; Jiang, J.; Luo, Y.; Zhang, G. Bridged Azobenzene Enables Dynamic Control of Through-Space Charge Transfer for Photochemical Conversion. *J. Phys. Chem. Lett.* **2021**, *12* (16), 3868-3874. DOI: 10.1021/acs.jpclett.1c00772.
68. Siewertsen, R.; Neumann, H.; Buchheim-Stehn, B.; Herges, R.; Näther, C.; Renth, F.; Temps, F. Highly Efficient Reversible Z−E Photoisomerization of a Bridged Azobenzene with Visible Light through Resolved S1(nπ*) Absorption Bands. *J. Am. Chem. Soc.* **2009**, *131* (43), 15594-15595. DOI: 10.1021/ja906547d.
69. Irie, M.; Fukaminato, T.; Sasaki, T.; Tamai, N.; Kawai, T. A digital fluorescent molecular photoswitch. *Nature* **2002**, *420* (6917), 759-760. DOI: 10.1038/420759a.
70. Heilemann, M.; Margeat, E.; Kasper, R.; Sauer, M.; Tinnefeld, P. Carbocyanine Dyes as Efficient Reversible Single-Molecule Optical Switch. *J. Am. Chem. Soc.* **2005**, *127* (11), 3801-3806. DOI: 10.1021/ja044686x.
71. van de Linde, S.; Sauer, M. How to switch a fluorophore: from undesired blinking to controlled photoswitching. *Chem. Soc. Rev.* **2014**, *43* (4), 1076-1087, 10.1039/C3CS60195A. DOI: 10.1039/C3CS60195A.
72. Li, H.; Vaughan, J. C. Switchable Fluorophores for Single-Molecule Localization Microscopy. *Chem. Rev.* **2018**, *118* (18), 9412-9454. DOI: 10.1021/acs.chemrev.7b00767.
73. Kashihara, R.; Morimoto, M.; Ito, S.; Miyasaka, H.; Irie, M. Fluorescence Photoswitching of a Diarylethene by Irradiation with Single-Wavelength Visible Light. *J. Am. Chem. Soc.* **2017**, *139* (46), 16498-16501. DOI: 10.1021/jacs.7b10697.
74. Gu, X.; Zhao, E.; Zhao, T.; Kang, M.; Gui, C.; Lam, J. W. Y.; Du, S.; Loy, M. M. T.; Tang, B. Z. A Mitochondrion-Specific Photoactivatable Fluorescence Turn-On AIE-Based Bioprobe for Localization Super-Resolution Microscope. *Adv. Mater.* **2016**, *28* (25), 5064-5071. DOI: https://doi.org/10.1002/adma.201505906 (acccessed 2023/09/22).
75. Tinnefeld, P.; Sauer, M. Molecular Optical Switches and Waveguides. *Optik & Photonik* **2007**, *2* (2), 45-48. DOI: https://doi.org/10.1002/opph.201190251 (acccessed 2023/09/22).
76. Tian, G.; Qiu, F.; Song, C.; Duan, S.; Luo, Y. Electric Field Controlled Single-Molecule Optical Switch by Through-Space Charge Transfer State. *J. Phys. Chem. Lett.* **2021**, *12* (37), 9094-9099. DOI: 10.1021/acs.jpclett.1c02578.
77. Seldenthuis, J. S.; van der Zant, H. S. J.; Ratner, M. A.; Thijssen, J. M. Electroluminescence spectra in weakly coupled single-molecule junctions. *Phys. Rev. B* **2010**, *81* (20), 205430. DOI: 10.1103/PhysRevB.81.205430.